

## Charging effects and the excitation spectrum of a quantum dot formed by an impurity potential

J. T. Nicholls, J. E. F. Frost, M. Pepper, D. A. Ritchie, M. P. Grimshaw, and G. A. C. Jones  
*Cavendish Laboratory, Madingley Road, Cambridge, CB3 0HE, United Kingdom*

(Received 24 May 1993)

We have studied Coulomb-blockade effects through a quantum dot formed by an impurity potential near a two-dimensional electron gas (2DEG) defined at a GaAs/Al<sub>x</sub>Ga<sub>1-x</sub>As heterojunction. We have compared the energy-level spacing within the quantum dot obtained by two methods: from the magnetic-field-induced gate-voltage shifts of the conductance peaks, and by applying a source-drain voltage across the dot. The use of the latter method in a magnetic field allows us to distinguish between charging and confinement effects, although the structure in the nonlinear excitation spectrum requires careful interpretation. As the number of electrons in the dot decreases, the barriers connecting the dot to the 2DEG thicken and the area of the dot decreases, giving rise to an increased charging energy that has been measured directly. After the final Coulomb-blockade conductance peak, we estimate that there are 20 electrons in the dot.

### INTRODUCTION

The Coulomb blockade (CB) of single-electron tunneling was first observed<sup>1</sup> in semiconductors in transport measurements through a quantum dot formed between impurities in a Si device. To gain some control and reproducibility over the CB effect, lithographically defined quantum dots similar to those first investigated by Smith *et al.*<sup>2</sup> were produced in a high-mobility two-dimensional electron gas (2DEG) formed at a GaAs/Al<sub>x</sub>Ga<sub>1-x</sub>As heterojunction.<sup>3</sup> In investigations of disordered systems, Coulomb-blockade oscillations have been observed<sup>4</sup> through dots which are formed when repulsive scattering centers have been deliberately introduced into a narrow one-dimensional channel to break the electron gas up into segments. In this paper we report the observation of CB conductance oscillations through a dot formed by an impurity near to the 2DEG, and controlled by a simple split-gate device defined over the GaAs/Al<sub>x</sub>Ga<sub>1-x</sub>As heterojunction. Although we do not have precise control over the height of the tunnel barriers in such a device, we shall show that the resulting quantum dot may contain fewer electrons than its lithographically defined counterparts. Before presenting the results we shall review how, if there are  $n$  electrons in the dot, the quantum confinement energies  $E_n$  modify the standard Coulomb charging picture.

In the classical picture of the Coulomb-blockade effect, an energy greater than  $e^2/C_\Sigma$  (where  $C_\Sigma$  is the total capacitance of the dot) is required to increase the charge on the dot by  $e$ . Transport through the dot is allowed when the Fermi energy  $E_F$  of the 2DEG is aligned with  $\mu$ , the chemical potential within the dot.  $\mu$  is proportional to the applied gate voltage  $V_g$ , and the change in gate voltage  $\Delta V_g$  that changes  $\mu$  by the charging energy is  $e\alpha\Delta V_g = e^2/C_\Sigma$ , where the constant of proportionality  $\alpha = C_g/C_\Sigma$ , and  $C_g$  is the capacitance between the dot and the gate. Therefore, periodic Coulomb-blockade conductance oscillations are observed with a voltage

spacing of  $\Delta V_g = e/C_g$ . When there is a small number of electrons in the dot, the energy spacing  $\Delta E_n = E_n - E_{n-1}$  between levels in the dot will modify the gate-voltage characteristics of the device. If the Coulomb term  $e^2/C_\Sigma$  is independent of  $E_n$ , the CB peaks are spaced by<sup>5</sup>

$$e\alpha\Delta V_g = e^2/C_\Sigma + \Delta E_n. \quad (1)$$

In contrast to  $e^2/C_\Sigma$ , the energy spacing  $\Delta E_n$  depends on the magnetic field  $B$ , and due to the sawtooth evolution<sup>6</sup> of the energy level  $E_n$  with magnetic field, the chemical potential  $\mu(n)$  of a dot containing  $n$  electrons will also vary in a sawtooth fashion. The magnetic-field dependence of CB peaks has been measured<sup>7</sup> in the quantum Hall effect regime. The peak positions were observed to oscillate in a sawtooth fashion as the field was increased; however, measurements<sup>7</sup> in the low-field regime ( $< 1$  T) showed random fluctuations in the position and amplitude of the peaks.

### SAMPLE DESCRIPTION

A split-gate device, with a width of  $0.3 \mu\text{m}$  and a length of  $0.3 \mu\text{m}$ , was lithographically defined on the surface of the sample,  $800 \text{ \AA}$  above the 2DEG. After brief illumination with a red light-emitting diode, the 2DEG had the following low-temperature properties: an electron concentration of  $5 \times 10^{10} \text{ cm}^{-2}$ , and a mobility estimated to be  $5 \times 10^4 \text{ cm}^2 \text{ V}^{-1} \text{ s}^{-1}$ . Because of the low carrier density, electrons are depleted from regions of the 2DEG under the gates even when they are at zero applied voltage. Due to the presence of impurities in the spacer layer above the 2DEG, spatial variations are induced in the bottom of the conduction band of the 2DEG.<sup>8</sup> We assume that one of these fluctuations near the split gate forms an attractive well where the electrons collect to create a quantum dot, and the number of electrons in the dot can be changed by varying the bias voltage on the split gate. Quantum dots have been measured in similar devices fabricated on the same wafer, though the dot

characteristics do vary from device to device, and from one cooldown to another. The results presented in this paper were all obtained from one particular sample, so that information derived from the different measurements could be compared.

Two-terminal differential conductance measurements  $G = dI/dV$ , using an ac excitation voltage of  $10 \mu\text{V}$ , were performed on the device in a dilution refrigerator. The magnetic field was applied perpendicular to the plane of the 2DEG. The total capacitance  $C_\Sigma$  of the dot is  $C_\Sigma = C_g + C_l + C_r$ , and if a dc source-drain voltage  $V_{sd}$  is applied to the dot the potential drop across each of the two tunnel barriers is electrostatically determined<sup>9</sup> by the capacitances,  $C_l$  and  $C_r$ , of the left and right tunnel barriers that separate the quantum dot from the 2DEG.

## RESULTS AND DISCUSSION

### Gate-voltage characteristics

Figure 1 shows the differential conductance  $G(V_g)$  through the dot measured as a function of the gate voltage  $V_g$  applied to one arm of the split gate, the other arm being kept at a constant voltage of  $-0.1 \text{ V}$ . Swapping the voltages applied to the two arms produced conductance oscillations similar to those in Fig. 1, leading us to believe that the dot is positioned equidistant from the two arms of the split gate. The sweeps were performed at various temperatures, and the different traces in Fig. 1 have been offset for clarity. The base temperature of 30 mK refers to the lattice temperature; the electrons themselves get no colder than 50–100 mK. Because the peaks have a tendency to drift slightly, we have labeled them no. 1, no. 2, etc., to denote their position with respect to the pinch-off voltage (a point just to the left of peak no. 1). The different peaks show a variety of behaviors as the temperature increases: the amplitudes of peaks no. 1 and no. 2 decrease, that of peak no. 3 increases, and peak no.

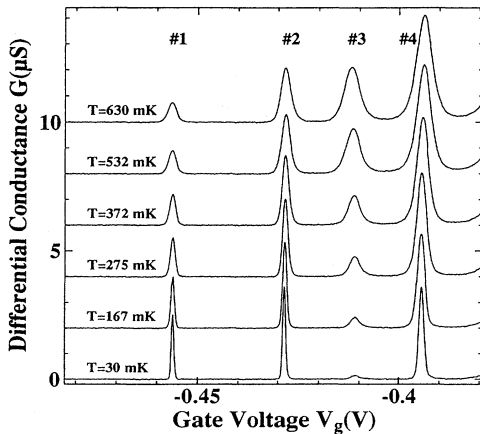


FIG. 1. Gate sweeps of the differential conductance  $G(V_g)$ , at base temperature and higher. The sweeps have been offset for clarity, and the peaks are labeled according to how close to pinch-off they occur.

4 has a roughly constant amplitude. Except for the anomalous voltage spacing between peaks no. 1 and no. 2, the CB peaks are fairly regularly spaced, with a separation that slowly increases as pinch-off is approached. Figure 2 shows conductance peaks nos. 15–27 measured in a magnetic field of  $B=4.4 \text{ T}$ . The magnetic field improves the periodicity of the peaks and lengthens the conductance zeros between adjacent peaks. A voltage spacing of  $\Delta V_g = 14 \text{ mV}$  can be clearly seen over a large gate-voltage range, from which we calculate  $C_g = 1.14 \times 10^{-17} \text{ F} = 11.4 \text{ aF}$ . Between the last two peaks  $C_g = 5.7 \text{ aF}$ .

Figure 3 shows the evolution of peak no. 1 as a function of the applied magnetic field; the sawtooth behavior associated with  $\Delta E_n(B)$  can be clearly observed in the low-field regime, occurring with a period  $\Delta B = 0.1 \text{ T}$ . As the field increases from zero, the position of the peak oscillates with an amplitude of about  $1 \text{ mV}$ . Accompanying this movement there is a modulation of the peak height. Using Eq. (1), we can compare the amplitude of the oscillation to the peak separation  $\Delta V_g$  to estimate the ratio  $\Delta E_n / (e^2 / C_\Sigma) \approx \frac{1}{30}$ . Using the value  $e^2 / C_\Sigma = 4.4 \text{ meV}$  from source-drain measurements (see later), we determine that the typical energy spacing is  $\Delta E_n = 150 \mu\text{eV}$ . For  $B < 0.7 \text{ T}$  (the field at which the first Shubnikov–de Haas oscillation appears) our data show peak shifts when there are no edge states in the 2DEG. This is in contrast to the data of McEuen *et al.*,<sup>7</sup> where edge states both inside and outside the dot are required to describe their results.

To observe the shifts in  $V_g$  associated with the energy spectrum requires the thermal broadening ( $\sim kT$ ) of the conductance peak to be much less than the energy spacing  $\Delta E_n$ . Previous studies<sup>3</sup> have shown that a CB peak centered at gate voltage  $V_0$  can be fitted to the line shape  $G \sim \text{sech}^2[\alpha e(V_g - V_0)/2kT]$  that describes<sup>10</sup> resonant tunneling through an isolated energy level in the dot. However, the temperature dependence of the amplitudes can show varied behavior,<sup>3,11</sup> similar to those observed in Fig. 1. Rather than changing  $kT$  relative to a fixed  $\Delta E_n$ ,

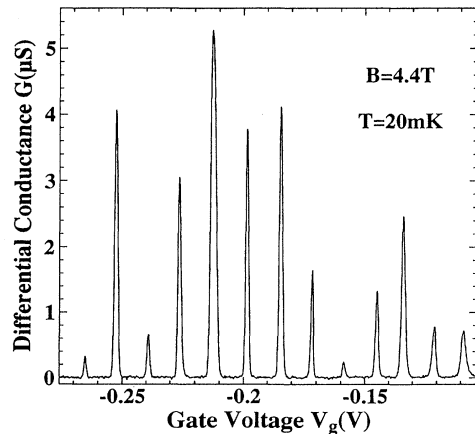


FIG. 2. Gate sweep of the differential conductance  $G(V_g)$  at  $V=4.4 \text{ T}$ , showing CB peaks nos. 15–27.

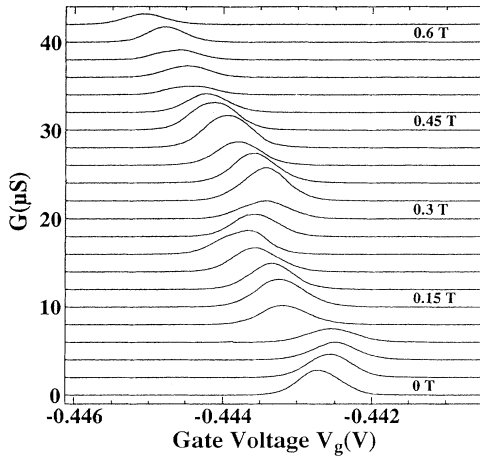


FIG. 3. The evolution of the differential conductance  $G(V_g)$  of CB peak no. 1 as the magnetic field is incremented in steps of 0.03 T. Successive traces have been displaced up the figure by 2  $\mu\text{S}$ .

Fig. 3 shows the use of a magnetic field to tune the relative separation of the energy levels at constant temperature  $T$ . The line shape varies as the Fermi energy  $E_F$  of the 2DEG changes from being close to just one energy level in the dot, to being close to more than one level. Figure 4(a) shows in more detail the conductance peak at

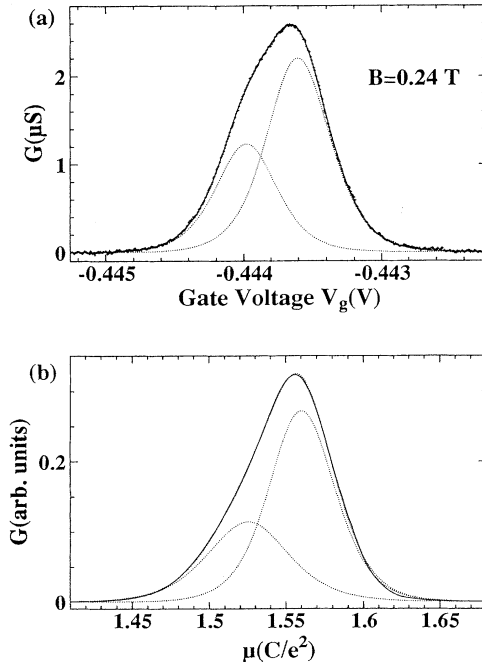


FIG. 4. (a) An expanded view of the conductance peak at  $B=0.24$  T in Fig. 3. The line shape has been fit with two functions each of the form  $G \sim \text{sech}^2[\alpha e(V_g - V_0)/2kT]$ , displaced from one another by 0.38 mV in gate voltage. (b) The calculated conductance  $G(\mu)$  as a function of the chemical potential in the dot, where conduction through the dot occurs via two energy levels. The transmission probabilities are  $\Gamma_1=0.8$  and  $\Gamma_2=0.1$ ; the other parameters (in units of  $e^2/C$ ) are  $kT=0.015$ ,  $E_1=0.0$ , and  $E_2=0.06$ .

$B=0.24$  T, which corresponds to the case where the thermal broadening is comparable to the spacing between two adjacent energy levels,  $E_1$  and  $E_2$ . Due to the Coulomb interaction, only one electron can pass through the dot at a given time. On the time scale of the measurement there are contributions due to current flowing through both energy levels, giving rise to the observed doublet. The experimental doublet in Fig. 4(a) is indistinguishable from the sum of two  $\text{sech}^2$  functions, displaced from one another by 0.38 mV in gate voltage, a separation that is equivalent to an energy spacing comparable to the thermal broadening of the Fermi energy at an electron temperature of 100 mK.

To show that such a doublet is physically reasonable, we have used the master formula [Eq. (3.14) in Ref. 10] to calculate the conductance as a function of the chemical potential  $\mu$  in the dot (and hence proportional to  $V_g$ ) for the case when there are just two isolated single-particle energies,  $E_1$  and  $E_2$ , in the dot. The conductance line shape is given by

$$G(\mu) = \frac{e^2}{kT} \sum_{p=1}^2 \sum_{N=1}^2 \frac{\Gamma_p^l \Gamma_p^r}{\Gamma_p^l + \Gamma_p^r} P_{\text{eq}}(N) F_{\text{eq}}(E_p | N) \times \{1 - f[E_p + U(N) - U(N-1) - \mu]\}, \quad (2)$$

where  $\Gamma_p^{(r,l)}$  are the tunneling rates of level  $p$  through the right/left tunnel barriers,  $P_{\text{eq}}(N)$  is the probability that the dot contains  $N$  electrons in equilibrium, and  $F_{\text{eq}}(E_p | N)$  is the conditional probability that level  $p$  is occupied given that the dot contains  $N$  electrons.  $f(x)$  is the usual Fermi function

$$f(x) = \left[ 1 + \exp\left\{\frac{x}{kT}\right\} \right]^{-1}, \quad (3)$$

and  $U(N)$  is the electrostatic energy required to put  $N$  electrons onto the dot. The transmission through the two levels is given by  $\Gamma_1 = \Gamma_1^l \Gamma_1^r / (\Gamma_1^l + \Gamma_1^r) = 0.8$  and  $\Gamma_2 = \Gamma_2^l \Gamma_2^r / (\Gamma_2^l + \Gamma_2^r) = 0.1$ , and (in units of  $e^2/C$ ):  $kT=0.015$ ,  $E_1=0.0$ , and  $E_2=0.06$ . Figure 4(b) shows the calculated conductance  $G(\mu)$  that peaks when there are  $\dots 1 \rightarrow 2 \rightarrow 1 \rightarrow 2 \rightarrow 1 \dots$  electrons on the dot. The resulting doublet can be fit (like the experimental data) to the sum of two  $\text{sech}^2$  resonant tunneling line shapes, each of approximate width  $kT$ , and spaced  $0.035(e^2/C)$  apart.

Weis *et al.*<sup>11</sup> obtained results that suggest that pairs of adjacent CB peaks show similar field-induced peak shifts; such an observation would result from the spin degeneracy of the levels within the dot. Our data do not show this effect, one possible explanation being that, towards pinch-off, the dot is shrinking and the confinement energies within the dot are changing so rapidly that the effect of spin degeneracy is masked.

At higher fields (2–4 T) the gate-voltage variations become less frequent, occurring with a period  $\Delta B \sim 0.3\text{--}0.5$  T and with a stronger modulation of the amplitude. The former observation is consistent with simple models<sup>6</sup> of the energy spectrum  $E_n(B)$  within the

dot, and the latter effect can be explained by different couplings between edge states inside and outside the dot.

#### Source-drain voltage measurements

By the addition of a dc source-drain voltage  $V_{sd}$  to the ac excitation voltage, it is possible to detect the energy states of the dot as they pass through the energy window,  $eV_{sd} = \mu_l - \mu_r$ , defined between the electrochemical potentials  $\mu_l$  and  $\mu_r$  of the left- and right-hand reservoirs.<sup>12</sup> Measurements of  $G(V_g)$  in Fig. 4 show the splitting of CB peak no. 1, as  $V_{sd}$  is incremented by  $55 \mu\text{V}$  between each gate-voltage sweep. To show the linear splitting of the original peak into two outer peaks, successive sweeps have been displaced up the figure by  $1.5 \mu\text{S}$ . The outer two peaks mark the positions where  $\mu(n)$  (the electrochemical potential of the ground state of the dot containing  $n$  electrons) passes through  $\mu_l$  and  $\mu_r$ . In comparison to previous experiments<sup>12,13</sup> we have measured peaks in  $G = dI/dV_{sd}$ , rather than steps in the current  $I(V_g)$ . Because the splitting of the peak (see Fig. 5) to positive and negative gate voltages is about the same, the voltage is dropped across the two barriers in roughly equal proportions, and hence the capacitances of the left and right barriers are approximately equal,  $C_r \approx C_l$ . As well as measuring the charging energies, the source-drain voltage also probes the excitation energies  $E_{n+1}^*$  within the dot. The excited states with  $n+1$  electrons on the dot are given by  $\mu(n) + E_{n+1}^*$ , and provided the condition  $\mu_l < \mu(n) < \mu_r$  is satisfied the excited states  $E_{n+1}^*$  within the energy window  $eV_{sd}$  can also be observed.<sup>12</sup> The negative differential conductance (noticeable near the right-hand outer peak) and the structure seen between the two

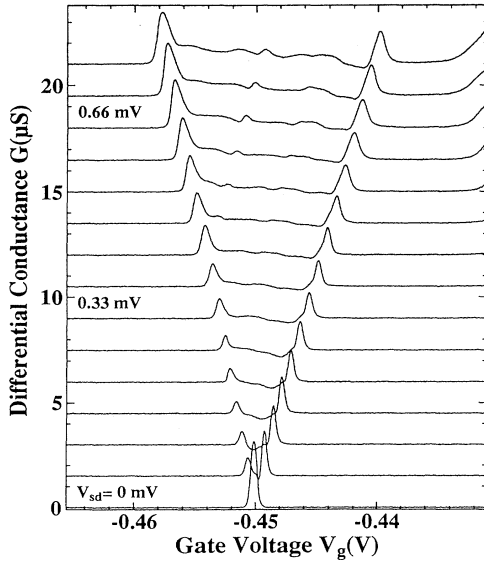


FIG. 5. Splitting of conductance peak no. 1 as the source-drain voltage  $V_{sd}$  is incremented by  $55 \mu\text{V}$  between sweeps. Successive traces of  $G(V_g)$  have been displaced up the figure by  $1.5 \mu\text{S}$ .

outer peaks are evidence of energy states within the dot. As  $V_{sd}$  is increased, structure emanates from the left-hand outer peak at intervals of  $50\text{--}150 \mu\text{V}$ —these voltage intervals are a measure of the energy spacing  $\Delta E_n$  in the dot.

Figure 6 shows source-drain voltage sweeps of the differential conductance  $G(V_{sd})$ , for gate voltages around the last few observable CB peaks. The successive sweeps have been displaced up the figure as  $V_g$  is decremented in steps of  $1.3 \text{ mV}$ . The regions of zero conductance centered about  $V_{sd} = 0$  are the Coulomb gaps, where the energy  $eV_{sd}$  is insufficient to put an extra electron onto the dot. The boundaries of the Coulomb gaps are surrounded by a peak in the differential conductance (a step in  $I-V_{sd}$ ), where current flow is no longer impeded. Assuming that  $e^2/C_\Sigma \gg \Delta E_n$ , the charging energy  $U = e^2/C_\Sigma$  is the width of the Coulomb gap. The charging energies measured from Fig. 6 are  $u_{0,1} > 6 \text{ meV}$ ,  $U_{1,2} = 4.4 \text{ meV}$ ,  $U_{2,3} = 2 \text{ meV}$ , and  $U_{3,4} = 1.4 \text{ meV}$ , where  $U_{n,n+1}$  is measured between the  $n$ th and  $(n+1)$ th labeled CB peaks. The corresponding capacitances  $C_{\Sigma 0,1} < 0.027 \text{ fF}$ ,  $C_{\Sigma 1,2} = 0.036 \text{ fF}$ ,  $C_{\Sigma 2,3} = 0.08 \text{ fF}$ , and  $C_{\Sigma 3,4} = 0.11 \text{ fF}$  decrease towards pinch-off. The temperature dependence of the zeros between the conductance peaks corroborates the observation that the total capacitance  $C_\Sigma$  decreases towards pinch-off. Figure 1 shows the differential conductance  $G(V_g)$  measured at temperatures up to  $640 \text{ mK}$ . The zeros between adjacent CB peaks depend on the ratio  $(e^2/C_\Sigma)/k_B T$ , and due to the decrease of  $e^2/C_\Sigma$  on going to more positive  $V_g$  the conductance zeros in Fig. 1 show an increasing sensitivity to temperature.

The straight lines defining the boundaries of the Coulomb gap show that the charging of the dot can be described by a model that was originally developed<sup>5</sup> for

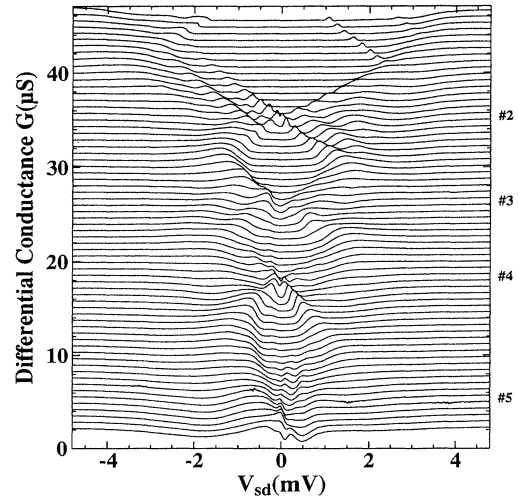


FIG. 6. Source-drain sweeps of the differential conductance  $G(V_{sd})$  as  $V_g$  is incremented in steps of  $1.3 \text{ mV}$  between sweeps. The labels on the right-hand side mark the gate-voltage positions of the conductance peaks at  $V_{sd} = 0$ .

metallic systems. The gap regions are parallelogram rather than rhombus in shape, reflecting the fact that  $C_1$  and  $C_r$  differ slightly and that the measurement circuit is itself asymmetric.<sup>11</sup> Assuming that  $C_g = 5.7$  aF and  $C_1 \approx C_r$ , we measure  $C_r = C_l = 15.3$  aF for the gap between CB peaks no. 1 and no. 2.

From the increasing size of the Coulomb gap towards pinch-off we measure directly a rapid reduction in the total capacitance  $C_\Sigma$  of the dot. A similar decrease of  $C_\Sigma$  due to the preferential thickening of one of the barriers towards pinch-off has been observed by Foxman *et al.*<sup>13</sup> in a moderate magnetic field. In our case, there is a thickening of both barriers as  $V_g$  becomes more negative, causing the wave function in the dot to shrink away from the 2DEG, decreasing  $C_1$  and  $C_r$  simultaneously. The dramatic increase in the barrier thicknesses causes a decrease in the size of the dot, resulting in a decrease of  $C_g$  (and the observed increase in  $\Delta V_g$ ) as pinch-off is approached. If we assume that the capacitance of the dot is that of an isolated disk,  $C_\Sigma = 4\epsilon_0\epsilon_r d$  (where  $d$  is the diameter of the dot and  $\epsilon_r = 12$  for GaAs), the charging energy  $e^2/C_\Sigma$  near pinch-off gives a dot diameter,  $d = 0.08$   $\mu\text{m}$ , and the number of electrons in the dot,  $n = 3$  (from the carrier density multiplied by the dot area) that are both unbelievably small. A more reasonable approximation for the number of electrons in the dot is given by the ratio  $2E_F/\Delta E_n \approx 20$  electrons. The discrepancies suggest that calculating the diameter from  $C_\Sigma = 4\epsilon_0\epsilon_r d$  is not reliable, and that there is probably an attractive potential causing the local carrier concentration to be higher in the dot than in the 2DEG.

Figure 7 shows a close-up of the Coulomb gap between peaks no. 1 and no. 2. The differential conductance measured in the negative bias direction shows stronger structure than that measured in the positive direction; this reflects the asymmetry of the two tunnel barriers.<sup>14</sup> Al-

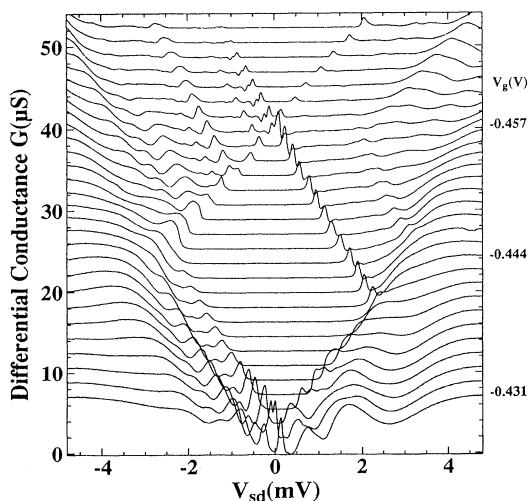


FIG. 7. Close-up of Fig. 6, showing in more detail the structure outside the last measurable Coulomb gap. The step size in  $V_g$  is 1.3 mV.

though the capacitances of the two tunnel barriers,  $C_1$  and  $C_r$ , are roughly equal, the asymmetry of the source-drain data probably reflects an asymmetry in the resistances of the two tunnel barriers. Outside the gap some structure is observed with a spacing of 100–200  $\mu\text{V}$ , whereas other structure occurs with a much larger spacing of  $\sim 0.5$  mV.

In order to distinguish between the different structures beyond the gap, the trace of  $G(V_{sd})$  at  $V_g = -0.457$  V in Fig. 7 has been measured as a function of magnetic field. The lowest trace in Fig. 8 was measured at  $B = 0$  T, and the evolution of the structure as the magnetic field is incremented in steps of 0.025 T is seen in the traces that are vertically displaced up the figure. The overall increase of the gap size is due to a slow gate-voltage drift of the position of the conductance peaks over the course of the experiment (1–2 days). In the classical picture the Coulomb gap  $U_{n,n+1}$  is independent of magnetic field; however, if the confinement energies are taken into account the measured Coulomb gap will be  $e^2/C_\Sigma + \Delta E_n(B)$ , which has some magnetic-field dependence. Close inspection of Fig. 8 shows small changes in the position of the first peak in the negative bias direction, marking the onset of conduction at the gap. These variations have an amplitude ( $\Delta E_n = 150$   $\mu\text{V}$ ) and period ( $\Delta B = 0.1$  T), which are in good agreement with the values obtained from Fig. 3.

In contrast to the small period ( $\Delta B = 0.1$  T) oscillations

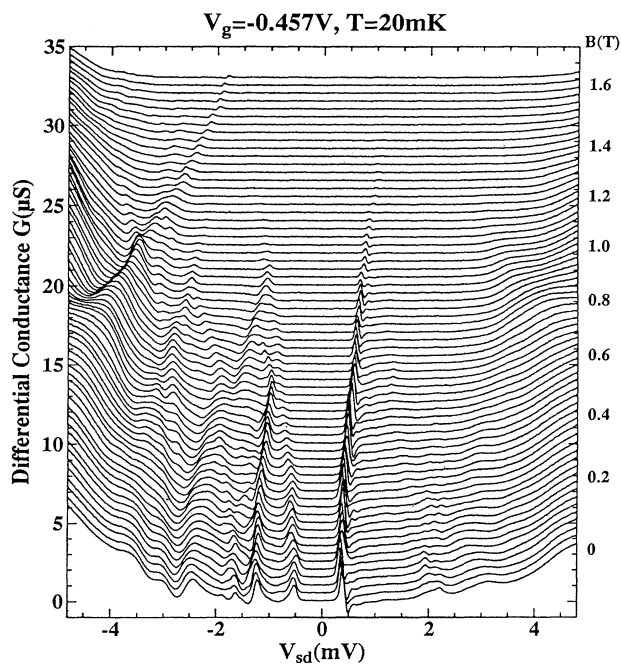


FIG. 8. Source-drain sweeps of the differential conductance  $G(V_{sd})$  at a fixed gate voltage,  $V_g = -0.457$  V, as a function of magnetic field from 0 to 1.65 T. The lowest trace was measured at 0 T, and successive traces (offset in the vertical direction) show the evolution of the conductance as  $B$  is incremented in steps of 0.025 T.

of  $\Delta E_n(B)$ , the strong features in Fig. 8 show variations that occur on a larger field scale. For example, large conductance peaks in the negative bias direction converge at 0.7 and 1.1 T. One of the uncertainties surrounding source-drain measurements<sup>11–13</sup> on lateral dots is whether the device can endure such large voltages without breaking down. This is especially true in our system where the Fermi energy is small and the tunnel barriers separating the dot from the 2DEG are not defined by gates. An alternative measure of the increasing Coulomb charging energy towards pinch-off is provided by the temperature dependence of the zeros between the conductance peaks. However, we have no such simple check for the structure measured beyond the gap. By using an ac excitation voltage of 50  $\mu\text{V}$ , or by increasing the temperature to 0.6 K, the strong structure in Fig. 8 remained unaffected, whereas the fine structure that we attribute to  $\Delta E_n(B)$  could no longer be resolved.

Evidence that breakdown is not occurring comes from our ability to distinguish charging effects beyond the gap that are not field dependent. Careful examination of Fig. 8 shows that the energy required to put a second electron onto the dot is independent of the magnetic field. At zero magnetic field this process occurs at  $-2.8$  mV, and at 1.1 T it has followed the shift of the gap and occurs at  $-3.2$  mV. Relative to the onset of conduction at the gap edge, it costs  $\sim 2$  meV ( $\approx U_{2,3}$ ) to put the second extra electron onto the dot.

If breakdown does not occur, then the nonlinear struc-

ture observed here and by others<sup>12</sup> requires some theoretical explanation.

## CONCLUSIONS

In conclusion, we have shown that a quantum dot formed at an impurity behaves as a controlled system that contains a small number of electrons. We have demonstrated that even at low magnetic fields the confinement energy-level spacing  $\Delta E_n(B)$  can be determined from the magnetic-field-induced shifts of the conductance peaks. As the field is increased the line shape of the conductance peak evolves in a manner that depends on the relative separation of the energy levels in the dot. The same energy spacing  $\Delta E_n(B)$  can be observed as variations of the Coulomb gap. However, measurements beyond the gap show structure with a magnetic dependence on a different field scale and that appears not to be related to the addition spectrum measured in low bias measurements. Although the origin and structure of our dot are not clear, our nonlinear results are similar to those obtained by Johnson *et al.*<sup>12</sup> on a defined dot.

## ACKNOWLEDGMENTS

This work was supported by the U.K. Science and Engineering Research Council. J.T.N. acknowledges support from the Isaac Newton Trust.

<sup>1</sup>J. H. F. Scott-Thomas, S. B. Field, M. A. Kastner, H. I. Smith, and D. A. Antoniadis, Phys. Rev. Lett. **62**, 583 (1989).

<sup>2</sup>C. G. Smith, M. Pepper, H. Ahmed, J. E. F. Frost, D. G. Hasko, D. C. Peacock, D. A. Ritchie, and G. A. C. Jones, J. Phys. C **21**, L893 (1988).

<sup>3</sup>U. Meirav, M. A. Kastner, and S. J. Wind, Phys. Rev. Lett. **65**, 771 (1990).

<sup>4</sup>A. A. M. Staring, H. van Houten, C. W. J. Beenakker, and C. T. Foxon, Phys. Rev. B **45**, 9222 (1992).

<sup>5</sup>For a review, see H. van Houten, C. W. J. Beenakker, and A. A. M. Staring, in *Single Charge Tunneling*, edited by H. Grabert and M. H. Devoret (Plenum, New York, 1992).

<sup>6</sup>See, for example in Ref. 5, the energy spectrum of a quantum dot with a two-dimensional parabolic confinement potential  $V(r) = m\omega^2 r^2/2$ .

<sup>7</sup>P. L. McEuen, E. B. Foxman, U. Meirav, M. A. Kastner, Y.

Meir, N. S. Wingreen, and S. J. Wind, Phys. Rev. Lett. **66**, 1926 (1991).

<sup>8</sup>J. H. Davies and J. A. Nixon, Phys. Rev. B **39**, 3423 (1989).

<sup>9</sup>H. Grabert, Z. Phys. **85**, 319 (1991).

<sup>10</sup>C. W. J. Beenakker, Phys. Rev. B **44**, 1646 (1991).

<sup>11</sup>J. Weis, R. J. Haug, K. v. Klitzing, and K. Ploog, Phys. Rev. B **46**, 12 837 (1992).

<sup>12</sup>A. T. Johnson, L. P. Kouwenhoven, W. de Jong, N. C. van der Vaart, C. J. P. M. Harmans, and C. T. Foxon, Phys. Rev. Lett. **69**, 1592 (1992).

<sup>13</sup>E. B. Foxman, P. L. McEuen, U. Meirav, N. S. Wingreen, Y. Meir, P. A. Belk, N. R. Belk, M. A. Kastner, and S. J. Wind, Phys. Rev. B **47**, 10020 (1993).

<sup>14</sup>D. V. Averin, A. N. Korotkov, and K. K. Likharev, Phys. Rev. B **44**, 6199 (1991).